

1 Laboratory #8: Computer-Generated Holograms

(OPTIONAL)

1.1 Theory:

In this lab, you will create “holographic” images of synthetic objects. These “computer-generated holograms” (or CGHs) are mappings of the complex amplitude (magnitude AND phase) of light reflected from or transmitted by synthetic objects. The wavefronts that would emerge from the objects are “reconstructed” by the propagation of light through the hologram. Holography is based on the “diffraction” of light by an object, which may be viewed as a result of Huygens’ principle that light propagates by creating spherical “wavelets”. A hologram is the record of the interference pattern generated by the wavefront from an object and from a known source (the *reference*). Holography was first described by Gabor in the 1940s, but did not become practical until lasers that produced (nearly) monochromatic light became available in the 1960s. The modifications to the holographic process that were first implemented by Leith and Upatniaks vastly improved the process and allowed 3-D objects to be reconstructed.

The description of a hologram is based on the theory of optical diffraction, which is specified in three regions that differ in their distance from the source (object). The three classes of diffraction region are:

1. Rayleigh-Sommerfeld diffraction: the light is considered to propagate exactly via spherical waves. The evaluated result is valid at any distance from the source, but the calculations are very difficult.
2. Fresnel diffraction: light is modeled as a paraboloidal wave (i.e., a quadratic-phase function), valid at a plane located a larger distance z_1 from the source. In this case, the propagation of light from a 2-D source function $f[x, y]$ over the distance z_1 is the convolution with the parabolic impulse response $h[x, y; z_1, \lambda_0]$, where z_1 and λ_0 are parameters of the “system:”

$$h[x, y; z_1, \lambda_0] = \frac{1}{i\lambda_0 z_1} \cdot \exp\left[+2\pi i \frac{z_1}{\lambda_0}\right] \cdot \exp\left[+i\pi \frac{x^2 + y^2}{\lambda_0 z_1}\right]$$

The term $(i\lambda_0)^{-1}$ is a phase term that is required for normalization; the factor z_1^{-1} is the approximation of the inverse square law in the Fresnel diffraction region; the factor $\exp\left[+2\pi i \frac{z_1}{\lambda_0}\right]$ is a constant phase term due to the propagation for the source plane to the observation plane, and the last (and most significant) term $\exp\left[+i\pi \frac{x^2 + y^2}{\lambda_0 z_1}\right]$ is a correction to the phase due to the off-axis location of the observation point. If the object function is a set of point sources (with the same wavelength λ_0) located in the plane specified by $z = 0$, the “image” of the diffracted light is the superposition of replicas this impulse response for each source point. We can specify the object distribution by a 2-D function $f[z, y; z = 0, \lambda_0]$ and the resulting superposition $g[x, y; z_1, \lambda_0]$ at the observation plane may be written as a convolution of the source function with this impulse response

$$\begin{aligned} g[x, y; z_1, \lambda_0] &= f[x, y; z = 0, \lambda_0] * h[x, y; z_1, \lambda_0] \\ &\equiv \frac{1}{i\lambda_0 z_1} \cdot \exp\left[+2\pi i \frac{z_1}{\lambda_0}\right] \iint_{-\infty}^{+\infty} f[\alpha, \beta; z = 0, \lambda_0] \cdot \exp\left[+i\pi \frac{(x - \alpha)^2 + (y - \beta)^2}{\lambda_0 z_1}\right] d\alpha d\beta \end{aligned}$$

where $[\alpha, \beta]$ are dummy variables of integration.

3. Fraunhofer diffraction: diffracted light is modeled as a plane wave; this approximation is valid only at observation planes located at a very large distance from the object or source. In this

case, the diffraction pattern $g[x, y; z_1, \lambda_0]$ produced by the 2-D input $f[x, y]$ is the 2-D Fourier transform with appropriately scaled coordinates

$$g[x, y] \propto F \left[\frac{x}{\lambda_0 z_1}, \frac{y}{\lambda_0 z_1} \right], \text{ where } \mathcal{F}_2 \{f[x, y]\} = F[\xi, \eta]$$

This experiment will consider holography in the Fraunhofer diffraction region only. We first consider the mathematical description of a simple hologram created by two point sources in the Fraunhofer diffraction region. It then concludes with a process for calculating the pattern for a simple hologram that you will create, print, and reconstruct. In your report of the experiment, you might also model the steps in the holographic process described in the next section.

1.2 Hologram of Two Point Sources in Fraunhofer Diffraction Region

The mathematical description of the holographic process evaluated in the Fraunhofer diffraction region is straightforward because of the Fourier transform relationship between the input source function and the diffracted amplitude. Consider the simple case of two point sources that emit the same monochromatic wavelength λ_0 and that are located in the plane $z = 0$. For convenience, one source is located “on axis” (at $x = y = 0$) with unit amplitude, while the relative amplitude of the second (“off-axis”) source is $a e^{+i\phi_0}$, where a is a real number that measures the relative magnitude and ϕ_0 is the relative phase. For convenience in the discussion, we choose a to lie in the interval $0 \leq a \leq 1$ so that the off-axis source is “fainter” than the on-axis source, though this constraint is not essential. Note that if the relative phase $\phi_0 = 0$, the two sources are “in phase”, if $\phi_0 = \pm\pi$, then the two sources are “out of phase”, and if $\phi_0 = \pm\frac{\pi}{2}$, the sources are “in quadrature”. The 3-D mathematical expression for the source function is:

$$\begin{aligned} f[x, y; z] &= \delta[x, y, z] + a e^{+i\phi_0} \delta[x - x_0, y, z] e^{+i\phi_0} \\ &= (\delta[x, y] + a e^{+i\phi_0} \delta[x - x_0, y]) \delta[z] \end{aligned}$$

The radiation from these sources is observed at the plane defined by $z = z_1$, which is assumed to be sufficiently distant so that the spherical waves are suitably approximated by plane waves. In other words, the description of Fraunhofer diffraction is appropriate. In such a case, the observed amplitude $s[x, y; z = z_1]$ is proportional to the Fourier transform of the source function evaluated at suitably scaled coordinates:

$$\begin{aligned} s[x, y; z_1] &\propto \mathcal{F}_2 \{f[x, y; z]\} \Big|_{\xi = \frac{x}{\lambda_0 z_1}, \eta = \frac{y}{\lambda_0 z_1}} \\ &= \left(1 + a e^{+i\phi_0} e^{-2\pi i \left(\frac{x_0}{\lambda_0 z_1} \right) x} \right) 1 \left[\frac{x}{\lambda_0 z_1}, \frac{y}{\lambda_0 z_1} \right] \end{aligned}$$

The measurable quantity at the observation plane is the irradiance $|s[x, y; z_1]|^2$, which is proportional to:

$$\begin{aligned} |s[x, y; z_1]|^2 &\propto \left(1 + a e^{+i\phi_0} e^{-2\pi i \left(\frac{x_0}{\lambda_0 z_1} \right) x} \right) \left(1 + a e^{-i\phi_0} e^{+2\pi i \left(\frac{x_0}{\lambda_0 z_1} \right) x} \right) \\ &= (1 + a^2) + 2a \cos \left[2\pi \left(\frac{x_0}{\lambda_0 z_1} \right) x - \phi_0 \right] \\ &= (1 + a^2) \left(1 + \frac{2a}{1 + a^2} \cos \left[2\pi \left(\frac{x_0}{\lambda_0 z_1} \right) x - \phi_0 \right] \right) \\ &\equiv (1 + a^2) \left(1 + \frac{2a}{1 + a^2} \cos [2\pi \xi_0 x - \phi_0] \right) \end{aligned}$$

where $\xi_0 \equiv \frac{x_0}{\lambda_0 z_1}$ is the spatial frequency of the sinusoidal irradiance pattern observed at the plane $z = z_1$. This sinusoidal “grating” oscillates over the range of amplitudes $(1 + a^2) \pm 2a$, and therefore

its modulation is:

$$\begin{aligned}
m &\equiv \frac{\left(|s[x, y; z_1]|^2\right)_{\max} - \left(|s[x, y; z_1]|^2\right)_{\min}}{\left(|s[x, y; z_1]|^2\right)_{\max} + \left(|s[x, y; z_1]|^2\right)_{\min}} \\
&= \frac{[(1+a^2)+2a] - [(1+a^2)-2a]}{[(1+a^2)+2a] + [(1+a^2)-2a]} = \frac{2a}{1+a^2}
\end{aligned}$$

The irradiance at the observation plane may be concisely expressed as:

$$|s[x, y; z_1]|^2 \propto \frac{1}{2} (1 + m \cos [2\pi\xi_0 x - \phi_0])$$

The modulation is unity if the sources have equal amplitude ($a = 1$) and approaches $m \simeq 2a$ if the amplitude of the second source $a \rightarrow 0$.

The sinusoidal grating generated by light from the two sources conveys evidence of their mutual existence. The various measurable parameters of the grating (orientation, period, phase at the origin, and modulation) are determined by the physical properties of the point sources (orientation, separation, relative phase, and relative amplitude). A recording of the irradiance pattern (as on a photographic emulsion) preserves the evidence of these properties, but it would be desirable to find a method for “reconstructing” images of the sources from this recording. In other words, we would like to find an “inverse filter” for the process of generating the sinusoidal grating.

To find the “inverse filter” for the process, it is necessary to model the photographic process mathematically, including the photographic storage of the pattern. We all know that photographic emulsions record “negative” images of the irradiance distribution, which is more accurately called the scaled “complement” in this context, as the measureable parameter is the optical “transmittance” t , which is in the interval $0 \leq t \leq 1$ and thus is nonnegative. The recorded transmittance t is small where the irradiance $|s[x, y; z_1]|^2$ is large. If the recording is “linear”, then the transmittance is doubled if the irradiance is halved. We also assume that the emulsion is “thin” and records only the interference pattern produced in the plane of the emulsion. “Thick” holograms record interference patterns in three dimensions and their description requires further details.

Our goal is to process the emulsion to produce a “hologram” whose optical transmittance is a faithful rendition of the complement of the sinusoidal irradiance, including the period, orientation, initial phase, and modulation. In our simple model, we will assume that the hologram is processed so that exposure to the “average” irradiance (i.e., the “bias” of the grating) produces a transmittance $t[x, y; z_1] = \frac{1}{2}$, while the modulation of the transmittance $t[x, y; z_1]$ is identical to that of the original irradiance $|s[x, y; z_1]|^2$. The appropriate mapping function $u[|s[x, y; z_1]|^2]$ is the complement of the incident irradiance after scaling to half-unit bias:

$$\begin{aligned}
t[x, y; z_1] &= u[|s[x, y; z_1]|^2] = \left(|s|^2\right)_{\max} - |s[x, y; z_1]|^2 \\
&= \frac{1}{2} \left(1 - m \cos \left[2\pi \left(\frac{x_0}{\lambda_0 z_1}\right) x - \phi_0\right]\right) 1[y] \\
&\implies \frac{1}{2} (1 - \cos [2\pi\xi_0 x - \phi_0]) 1[y] \text{ for } a = 1 \\
&\implies \frac{1}{2} - a \cos [2\pi\xi_0 x - \phi_0] 1[y] \text{ for } a \simeq 0
\end{aligned}$$

where $\xi_0 \equiv \frac{x_0}{\lambda_0 z_1}$. This recorded pattern $t[x, y; z_1]$ is the hologram. In this case, it is a simple sinusoidal pattern along the x -axis and constant along y . Note also how simple this pattern was to calculate – this is the basis for the idea of computer-generated holography.

A side comment about “reality” is essential here. In real life, it is no simple task to develop the emulsion so that the transmittance is proportional to the scaled complement of the irradiance. Nonlinear deviations from this ideal behavior that complicate the analysis can easily “creep into” the processing. We will consider the qualitative effects of the nonlinearities after analyzing the ideal

result. Also, this example assumes that the holographic recording is infinitely large. Though this assumption seems to be unrealistic, it is no more so than the assumption of Fraunhofer diffraction itself, which is only valid within some region near the optical axis.

Now, replace the processed hologram in its original position and reilluminate it by light from the on-axis source. The illumination is a plane wave that travels down the z -axis. The action of the hologram is to modulate the source illumination to produce an amplitude pattern proportional to $t[x, y, z_1]$. The hologram is “reconstructed” by propagating this amplitude distribution to an observation plane “downstream” from the hologram. Consider that the propagation distance to the observation plane is z_2 , so that the amplitude is observed at the plane defined by $z = z_1 + z_2$. If z_2 is sufficiently large so that the Fraunhofer diffraction model is appropriate, then the output amplitude pattern is again proportional to the Fourier transform of the recorded transmittance pattern $t[x, y; z_1]$:

$$\begin{aligned}
g[x, y; z_1 + z_2] &\propto T[\xi, \eta] \Big|_{\xi = \frac{x}{\lambda_0 z_2}, \eta = \frac{y}{\lambda_0 z_2}} \\
&= \mathcal{F}_2 \left\{ \left(\frac{1}{2} - \frac{a}{1+a^2} \cos[2\pi\xi_0 x - \phi_0] \right) 1[y] \right\} \Big|_{\xi = \frac{x}{\lambda_0 z_2}, \eta = \frac{y}{\lambda_0 z_2}} \\
&\propto \frac{1}{2} \delta \left[\frac{x}{\lambda_0 z_2}, \frac{y}{\lambda_0 z_2} \right] \\
&\quad - \frac{1}{2} \frac{a}{1+a^2} \delta \left[\frac{1}{\lambda_0 z_2} \left(x + \frac{z_2}{z_1} x_0 \right), \frac{y}{\lambda_0 z_2} \right] e^{-i\phi_0} \\
&\quad - \frac{1}{2} \frac{a}{1+a^2} \delta \left[\frac{1}{\lambda_0 z_2} \left(x - \frac{z_2}{z_1} x_0 \right), \frac{y}{\lambda_0 z_2} \right] e^{+i\phi_0} \\
&= \frac{(\lambda_0 z_2)^2}{2} \left[\delta[x, y] - \frac{a}{1+a^2} \left(\delta \left[x + \frac{z_2}{z_1} x_0, y \right] e^{-i\phi_0} + \delta \left[x - \frac{z_2}{z_1} x_0, y \right] e^{+i\phi_0} \right) \right] \\
&\propto \delta[x, y] - \frac{a}{1+a^2} \left(\delta \left[x + \frac{z_2}{z_1} x_0, y \right] e^{-i\phi_0} + \delta \left[x - \frac{z_2}{z_1} x_0, y \right] e^{+i\phi_0} \right)
\end{aligned}$$

where the scaling property of the Dirac delta function has been applied. The output irradiance is proportional to the squared magnitude of this pattern, which squares the weighting factors of the Dirac delta functions:

$$\begin{aligned}
|g[x, y; z_1]|^2 &\propto \delta[x, y] + \left(\frac{a}{1+a^2} \right)^2 \left(\delta \left[x + \frac{z_2}{z_1} x_0, y \right] + \delta \left[x - \frac{z_2}{z_1} x_0, y \right] \right) \\
&= \delta[x, y] + \left(\frac{m}{2} \right)^2 \left(\delta \left[x + \frac{z_2}{z_1} x_0, y \right] + \delta \left[x - \frac{z_2}{z_1} x_0, y \right] \right)
\end{aligned}$$

where the real-valued character of a has been used. In words, this output “image” is a set of three Dirac delta functions: one “on axis” with “power” proportional to unity, and two separated from the origin by $x = \pm \frac{z_2}{z_1} x_0$ with “power” proportional to $\left(\frac{a}{1+a^2} \right)^2 = \left(\frac{m}{2} \right)^2$. The “reconstructed” image is a “magnified” replica of the autocorrelation of the source function that has been scaled in both position and . The intensity of the off-axis Dirac delta functions are scaled by $\frac{1}{4}$ if $a = 1$ and by approximately a^2 if $a \simeq 0$.

1.3 Equipment:

1. Computer running IDL (or other software tool that includes a random number generator and the discrete Fourier transform);
2. Transparency material for printing on copier/computer printer;
3. He:Ne Laser, optical bench, and optical components to reconstruct the image.

1.4 Procedure:

Adapted (i.e., stolen) from a procedure by Dr. William J. Dallas of the University of Arizona (??)

This method computes a “detour-phase” computer-generated hologram (CGH) using a multipixel cell to represent the complex amplitude of the Fourier transform of the object; each cell is an approximation of the complex-valued Fourier transform, which then may be placed in a beam of coherent light that propagates to the Fraunhofer diffraction region to evaluate the Fourier transform of the Fourier transform.

The method used here was originally implemented by Adolf Lohmann in the 1960s, and is particularly attractive because of it is both simple and yet also produces fairly good images of simple objects. Other variations of this method have also been implemented.

In the Lohmann hologram, an approximation of the complex-valued Fourier transform is displayed as a real-valued array of “bitonal” apertures. The pixels in the pattern can take on one of two values for the transmittance: “0” (opaque) or “1” (transparent). The algorithm encodes the Fourier transform of the object pattern, and thus assumes that the hologram is reconstructed by propagating the light to the Fraunhofer diffraction region, where diverging spherical wavefronts propagating from a point object may be approximated by plane waves. The object is assumed to be planar (2-D) because the light is assumed to propagate a large distance from the hologram (into the Fraunhofer diffraction region), so that the wavefronts are assumed to be planar. The difference in time required to travel 3-D objects may be modeled if the light diffracts into the Fresnel diffraction region.

In the detour-phase CGH, the 2-D Fourier transform is modeled as a real-valued array of bitonal apertures. The “size” and “position” of the apertures maps the magnitude and phase of the complex amplitude of the interference pattern that would be generated by the object points and the reference beam, respectively. The phase of the Fourier transform is generated by varying the “travel time” of the light by changing the position of the aperture.

1.4.1 Recipe for a Detour-Phase Hologram

The outcome of each step is illustrated using a 1-D object.

1. Create an $N \times N$ 2-D complex-valued array filled with zeros. The dimension of the array should be a power of two and *at least* as large as $N \geq 64$ (though I suggest setting $N = 512$, if possible) Index the array over the domain:

$$-\frac{N}{2} \leq n, m \leq +\frac{N}{2} - 1$$

2. Define a 2-D bitonal (“black and white”) object (e.g., an alphabetic character) over smaller square array, say $M \times M$, where $M = 64$ or even 128. The smaller array should be centered within the large array. Make the characters out of “white” pixels (level $f = 1$, unit magnitude) on a “black” background (level $f = 0$).
3. Use a uniformly distributed random-number generator to assign a random phase ϕ to each pixel from the interval:

$$-\pi \leq \phi < +\pi$$

Note that most language compilers include a random number generator with a uniform distribution over the interval $[0, 1)$, so the desired range is obtained by simple arithmetic:

$$\phi = \left(RAND - \frac{1}{2} \right) \cdot 2\pi$$

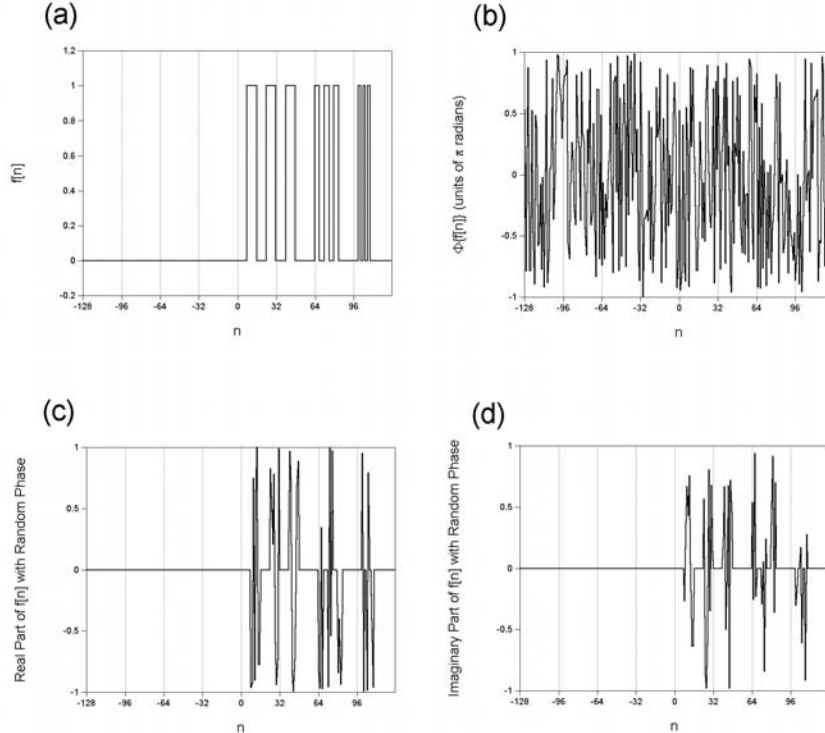
where $RAND$ is a pseudocode for the random number function. This random phase applied to each pixel has the effect of assuming that the reflecting object (the bitonal alphabetic character) reflects light with the same wavelength but a different phase; in other words, the resulting function approximates a “diffuse” reflecting object. The resulting complex-valued array $g[n, m]$ has the values:

$$\begin{aligned} g[n, m] &\equiv f[n, m] \cdot \exp \left[+i \left(RAND - \frac{1}{2} \right) \cdot 2\pi \right] \\ &= f[n, m] \cdot \cos \left[\left(RAND - \frac{1}{2} \right) \cdot 2\pi \right] + i f[n, m] \cdot \sin \left[\left(RAND - \frac{1}{2} \right) \cdot 2\pi \right] \end{aligned}$$

where $f[n, m]$ is the bitonal array containing the alphabetic character. The end result is the object function $g[n, m]$. The indices $[n, m]$ determine the spatial position in the array via the relationships:

$$\begin{aligned} x &= n \cdot \Delta x \\ y &= m \cdot \Delta y \end{aligned}$$

where $\Delta x, \Delta y$ are the intervals between samples along the two axes. For our purposes here, we may just think of $\Delta x = \Delta y = 1$ unit. An example for a 1-D function (3-bar chart modeled after the USAF resolution target) is shown in part (c) of the figure:



1-D simulation of detour-phase CGH: (a) bitonal object $f[x]$ consisting of sets of three “bars”; (b) random phase selected from uniform distribution over interval $-\pi \leq \phi < +\pi$; (c) $\Re\{f[x]\}$ with random phase; (d) $\Im\{f[x]\}$ with random phase.

4. Compute either the *discrete Fourier transform* (DFT) or its “fast” relative (FFT) of the 2-D “centered” complex-valued array $g[n, m]$; this produces a complex-valued array of two indices in the “frequency domain,” e.g., $G[k, \ell]$, where k and ℓ are the indices for the “spatial frequencies” of the sinusoidal components of $g[n, m]$. In other words, the spatial frequencies of the samples are:

$$\begin{aligned}\xi &= k \cdot \Delta\xi = k \cdot \frac{1}{N \cdot \Delta x} \\ \eta &= \ell \cdot \Delta\eta = \ell \cdot \frac{1}{N \cdot \Delta y}\end{aligned}$$

If $\Delta x = \Delta y = 1$ unit of length, then $\xi = \frac{k}{N}$ and $\eta = \frac{\ell}{N}$ “cycles per unit length.” For an $N \times N$ array of points $g[n, m]$, the DFT is defined to be:

$$\begin{aligned}G[k, \ell] &= \sum_{k=-\frac{N}{2}}^{\frac{N}{2}-1} \sum_{\ell=-\frac{N}{2}}^{\frac{N}{2}-1} g[n, m] \cdot \exp \left[-2\pi i \frac{(nk + m\ell)}{N} \right] \\ &= \sum_{k=-\frac{N}{2}}^{\frac{N}{2}-1} \sum_{\ell=-\frac{N}{2}}^{\frac{N}{2}-1} (\operatorname{Re} \{g[n, m]\} + i \operatorname{Im} \{g[n, m]\}) \cdot \left(\cos \left[2\pi i \frac{(nk + m\ell)}{N} \right] - i \cdot \sin \left[2\pi i \frac{(nk + m\ell)}{N} \right] \right) \\ &= \sum_{k=-\frac{N}{2}}^{\frac{N}{2}-1} \sum_{\ell=-\frac{N}{2}}^{\frac{N}{2}-1} \left(\operatorname{Re} \{g[n, m]\} \cdot \cos \left[+2\pi \frac{(nk + m\ell)}{N} \right] \right) - \left(\operatorname{Im} \{g[n, m]\} \cdot \sin \left[+2\pi \frac{(nk + m\ell)}{N} \right] \right) \\ &\quad + i \cdot \sum_{k=-\frac{N}{2}}^{\frac{N}{2}-1} \sum_{\ell=-\frac{N}{2}}^{\frac{N}{2}-1} \left(\operatorname{Im} \{g[n, m]\} \cdot \cos \left[+2\pi \frac{(nk + m\ell)}{N} \right] \right) - \left(\operatorname{Re} \{g[n, m]\} \cdot \sin \left[+2\pi \frac{(nk + m\ell)}{N} \right] \right) \\ \operatorname{Re} \{G[k, \ell]\} &= \sum_{k=-\frac{N}{2}}^{\frac{N}{2}-1} \sum_{\ell=-\frac{N}{2}}^{\frac{N}{2}-1} \left(\operatorname{Re} \{g[n, m]\} \cdot \cos \left[+2\pi \frac{(nk + m\ell)}{N} \right] \right) - \left(\operatorname{Im} \{g[n, m]\} \cdot \sin \left[+2\pi \frac{(nk + m\ell)}{N} \right] \right) \\ \operatorname{Im} \{G[k, \ell]\} &= \sum_{k=-\frac{N}{2}}^{\frac{N}{2}-1} \sum_{\ell=-\frac{N}{2}}^{\frac{N}{2}-1} \left(\operatorname{Im} \{g[n, m]\} \cdot \cos \left[+2\pi \frac{(nk + m\ell)}{N} \right] \right) - \left(\operatorname{Re} \{g[n, m]\} \cdot \sin \left[+2\pi \frac{(nk + m\ell)}{N} \right] \right)\end{aligned}$$

where the outputs are specified on the intervals:

$$-\frac{N}{2} \leq k, \ell \leq \frac{N}{2} - 1$$

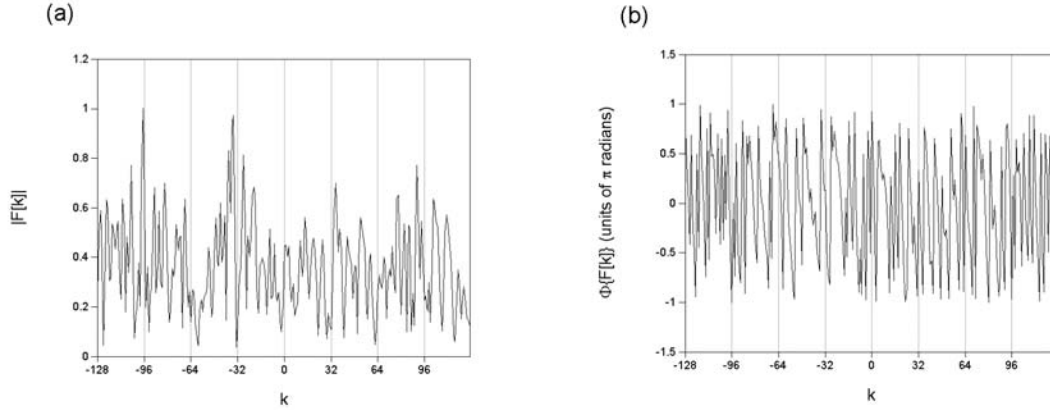
You can probably find precoded DFT and FFT routines available on the Internet. Note, however, that many FFT routines are defined over the discrete domain $[0 \leq n, k \leq N - 1]$ instead of $[-\frac{N}{2} \leq n, k \leq \frac{N}{2} - 1]$. In these cases, you can use the program if you “checkerboard” the input and output arrays (multiply alternate pixels by -1).

5. Compute the magnitude and phase of the 2-D FFT of the array $g[n, m]$:

$$G[k, \ell] = \operatorname{Re} \{G[k, \ell]\} + i \operatorname{Im} \{G[k, \ell]\}$$

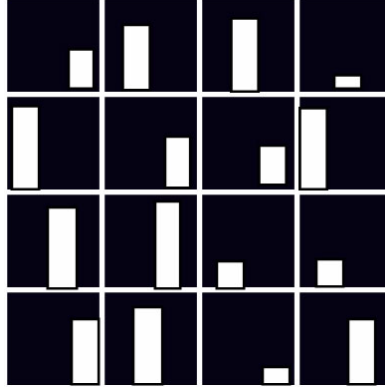
$$\begin{aligned}|G[k, \ell]| &= \sqrt{(\operatorname{Re} \{G[k, \ell]\})^2 + (\operatorname{Im} \{G[k, \ell]\})^2} \\ \Phi \{G[k, \ell]\} &= \tan^{-1} \left[\frac{\operatorname{Im} \{G[k, \ell]\}}{\operatorname{Re} \{G[k, \ell]\}} \right], \text{ where } -\pi \leq \Phi < +\pi\end{aligned}$$

The magnitude and phase of the DFT of the 1-D array shown before are displayed in the figure:



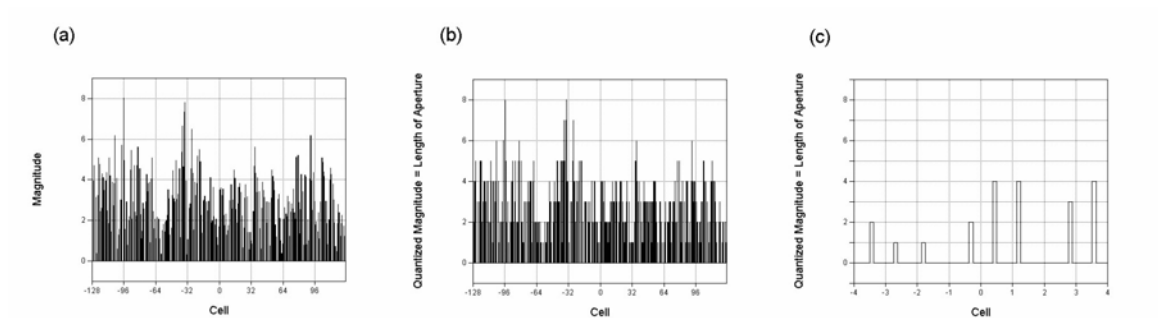
FFT $G[k]$ for 1-D object $g[n] = f[n] \cdot \exp[+i\phi[n]]$, where $\phi[n]$ is the random phase at pixel indexed by n : (a) magnitude $|G[k]| \geq 0$; (b) phase $-\pi \leq \Phi\{G[k]\} < +\pi$.

6. Normalize the magnitudes at each pixel by dividing by the maximum of all the magnitudes.
7. Select a cell size for the hologram; this is the size of the bitonal cell that will be used to approximate the complex amplitude (magnitude and phase) of each pixel in the Fourier transform array $G[k, \ell]$; I suggest trying 8×8 cells, but note that this enlarges your array by factors of 8 in each dimension (which should not be a problem).
8. Quantize the magnitudes so that the largest value is the linear dimension of your cell array, i.e., if you are using an 8×8 cell, multiply the normalized magnitude (so that $G_{\max} = 1$) by 8 and then round to the nearest whole number; this will produce integer values between 0 and 8.
9. Quantize the phase at each pixel by dividing by 2π , multiplying by the linear dimension of your cell, and rounding to the nearest whole number – this will produce phase numbers in the interval $[-4, +3]$.
10. Now for the trickiest part; we need to make bitonal apertures corresponding to each quantized magnitude and quantized phase for each pixel. The apertures take the form of transparent holes on an opaque background in each cell of size (at least) 8×8 pixels. With this cell size, the normalized magnitude is quantized to the interval $0 \leq |G_{\text{normalized}}[k, \ell]| \leq 8$ and the phase is in the interval $[-4, +3]$. The vertical “length” of the aperture in each cell is the quantized magnitude of that pixel in $G[k, \ell]$, while the horizontal “position” of the aperture is the quantized phase of the pixel $G[k, \ell]$. A 2-D example of the cells that might be obtained is shown in the figure:



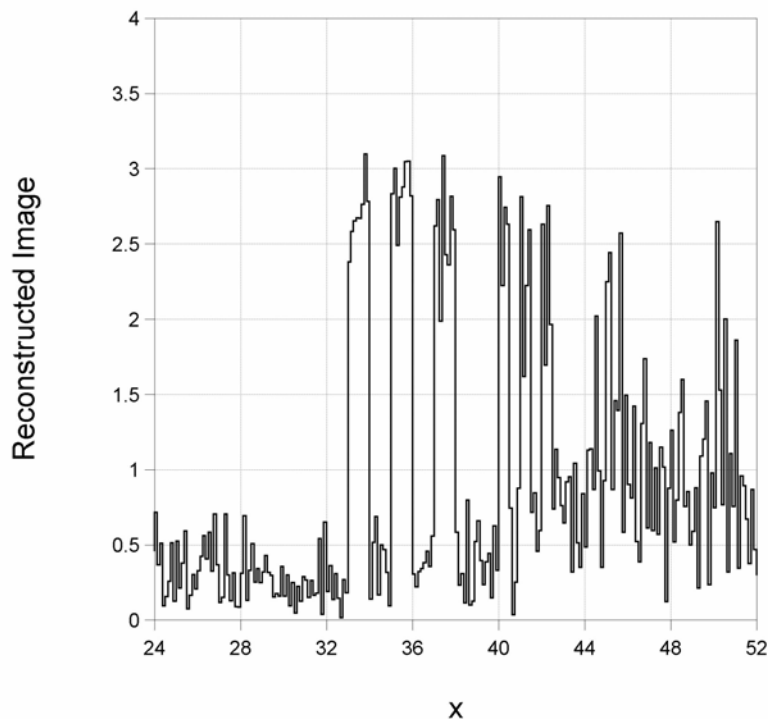
Example of the cell patterns that might be obtained for a particular CG hologram.

The results for the same 1-D example (3-bar target) is shown in the figure.



Output of CGH after rendering in cells: (a) showing cells with length proportional to the magnitude of each sample of $F[k]$; (b) after lengths of cells have been quantized to integer values between 0 and 8; (c) magnified view, showing that the apertures are located at different phases.

11. Print out the bitonal array with an electrophotographic laser or inkjet printer on overhead transparency film at a small size. If the printer is capable of 600 dpi, try printing at this scale and perhaps at 300 dpi.
12. Display the hologram by illuminating with a He:Ne laser and view in the Fraunhofer diffraction region (i.e., far “downstream” from the hologram). You may have to use a lens to move the Fraunhofer region closer to the object in exactly the same manner as in Laboratory #6 on Diffraction on #7 on Fourier optics.



Magnified view of reconstruction of 1-D hologram, showing sets of three bars in reconstructed image. The “noise” in the image is due to the quantized magnitude and phase.

This algorithm for evaluating the Fourier transform appears often in various imaging applications, and is particularly important in optics because optical propagation may be modeled as convolution with an appropriately scaled quadratic-phase function.

1.5 References

- Reynolds, G.O., J.B. DeVelis, G.B. Parrent, and B.J. Thompson, *The New Physical Optics Notebook*, SPIE, 1989.
- Iizuka, K. *Engineering Optics*, Springer-Verlag, 1984
- Dallas, W.J., “Computer-Generated Holograms”, §6 in *The Computer in Optical Research*, B.R. Frieden, Springer-Verlag, 1980.
- Collier, Robert J., C.B. Burckhardt, and L.H. Lin, *Optical Holography*, Academic Press, 1971.
- B.R. Brown and A.W. Lohmann, *Appl.Opt.*, **5**, 967, 1966.
- A.W. Lohmann and D.P. Paris, *Appl.Opt.*, **6**, 1739, 1967.
- R.L. Easton, Jr., R. Eschbach, and R. Nagarajan, *Error diffusion in cell-oriented holograms to compensate for printing constraints*, **Journal of Modern Optics** **43**(6), 1219-1236, 1996.